European Conference on Computational Fluid Dynamics
ECCOMAS CFD 2006
P. Wesseling, E. Oñate, J. Périaux (Eds)

NUMERICAL SIMULATION OF TRANSSKULL FOCUSED ULTRASOUND

Yusuke NAKAJIMA*, Yoshiaki TAMURA† and Yoichiro MATSUMOTO‡

*Toyo University,
2100 Kujirai, Kawagoe, Saitama,
Japan
e-mail: yusuke@cse.eng.toyo.ac.jp

† Toyo University,
2100 Kujirai, Kawagoe, Saitama,
Japan
e-mail: tamtam@eng.toyo.ac.jp

‡University of Tokyo,
7-3-1 Hongo, Bunkyo-ku, Tokyo,
Japan
e-mail: ymats@felt.t.u-tokyo.ac.jp

Key words: HIFU treatment, Transskull ultrasound propagation, CT scan

Abstract. *The focused ultrasound wave attracts attention in the medical field in various applications such as High Intensity Focused Ultrasound (HIFU). Amount of sound energy is generated by focused ultrasound in the body of narrow area. Present HIFU treatment cannot be applied to the part surrounded by bones, such as brain, because focal point is changed by refraction and reflection of ultrasound. In this research transskull ultrasound propagation is analyzed by finite difference method for HIFU treatment to brain. Assumption of isentropy and small disturbance of Euler equation gives the governing equation. The density and speed of sound of each medium are given at the center of Cartesian grid cells so as to model arbitrary human body from Computerized Tomography scan images. As wavelength of an ultrasound is very short, large amount of grid points is required. Therefore, parallel computing using MPI is performed.*

1 INTRODUCTION

The focused ultrasound wave attracts attention in the medical field in various applications. Amount of sound energy is generated by focused ultrasound in the body of narrow area[1]. It is converted to sound pressure and thermal energy for medical treatment, such as Extracorporeal Shock Wave Lithotripsy (ESWL), High Intensity Focused Ultrasound (HIFU) [2,3] and so on. In ESWL system, the strong sound pressure is generated by focused ultrasound and calculus is fractured by sound pressure. In HIFU system, the thermal energy is generated by focused ultrasound. Ultrasound is non-invasive and the treatment using focused ultrasound is suitable for medical application.

Present HIFU treatment is only used for superficial part such as prostate, breast and so on and cannot be applied to the part surrounded by bones, such as brain, because focal point is changed by refraction and reflection of ultrasound. In order to apply HIFU treatment to brain, we propose a simulation method to analyze focused ultrasound propagation.

In this research transskull ultrasound propagation is analyzed by finite difference method

for apply HIFU treatment to brain. Assumption of isentropy and small disturbance of Euler equation gives the governing equation. The density and speed of sound of each medium are given at the center of Cartesian grid cells so as to model arbitrary human body.

The data of human head would be input into computational grid by Computerized Tomography scan (CT scan) [4]. CT scan image is used to measure internal density of skull. Bone has various density and speed of sound. The skull has three-layered structure, structure of porous zone layer, and dense layers. Structure of porous zone is very inhomogeneous. Porosity map is directly linked to CT scan data, called Hounsfield value. Density map and speed of sound map of skull are deduced from porosity map[5].

As wavelength of an ultrasound is very short, large amount of grid points are required. Therefore, parallel computing using MPI is performed.

In the second section the numerical method and the scheme are described. In the third section is verification of the code by comparison with experiment is present. In the forth section simulated is two dimensional transskull focused ultrasound.

2 NUMERICAL METHOD

2.1 Computational grid

The data of human skull would input into computational grid by Computerized Tomography scan (CT scan). Then, Cartesian grid is used in order to simply input arbitrary shape of human skull. Equal-spacing grid is formed and used throughout the research.

As described in the next part, the density and the speed of sound represent a variation of media in a human body. The values of each medium (ρ and c) are given at the center of grid cells so as to simulate arbitrary organs in a human body.

2.2 Governing equation

A governing equation is derived from Euler equation as

$$\frac{\partial^2 p}{\partial t^2} = c^2 \rho \left[\frac{\partial}{\partial x}\left(\frac{1}{\rho}\frac{\partial p}{\partial x} \right) + \frac{\partial}{\partial y}\left(\frac{1}{\rho}\frac{\partial p}{\partial y} \right) + \frac{\partial}{\partial z}\left(\frac{1}{\rho}\frac{\partial p}{\partial z} \right) \right] \tag{1}$$

under assumption of isentropy and small disturbance where p is acoustic pressure field(scalar), t is time, $\rho(\vec{r})$ is the density, $c(\vec{r})$ is the speed of sound and, $\vec{r}$ is the position vector.

2.2 Computational grid

Equation (1) is discretized as

$$\frac{p^{n+1} - 2p^n + p^{n-1}}{(\Delta t)^2} = c^2{}_{jkl} \cdot p_{jkl} \left[\delta_x \left(\frac{1}{\rho_{jkl}} \cdot \delta_x p_{jkl} \right) + \delta_y \left(\frac{1}{\rho_{jkl}} \cdot \delta_y p_{jkl} \right) + \delta_z \left(\frac{1}{\rho_{jkl}} \cdot \delta_z p_{jkl} \right) \right]^{n+1} \tag{2}$$

where,

$$\delta_x f_{j,k,l} \equiv \frac{f_{j+1/2,k,l} - f_{j-1/2,k,l}}{\Delta x},$$
$$\delta_y f_{j,k,l} \equiv \frac{f_{j,k+1/2,l} - f_{j,k-1/2,l}}{\Delta y}, \qquad (3)$$
$$\delta_z f_{j,k,l} \equiv \frac{f_{j,k,l+1/2} - f_{j,k,l+1/2}}{\Delta z}.$$

Above equation is second order both in time and in space, and solved by SOR (Successive Over Relaxation) method.

3 VERIFICATION OF THE CODE

3.1 Problem setup

A test problem is shown in Fig. 1. A rectangular obstacle is set in water to observe the reflection and refraction of ultrasound. Calculation area was 66mm × 66mm.

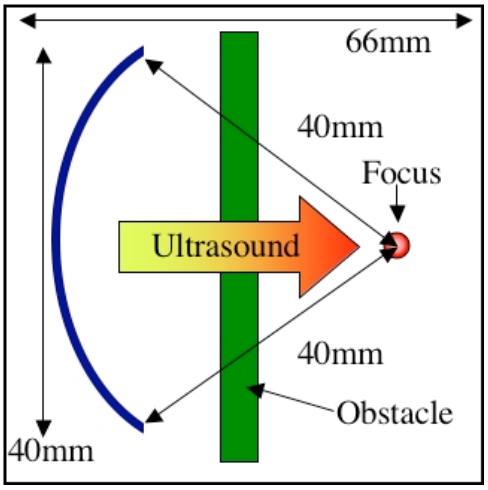

Figure 1: Test problem

3.2 Numerical result for verification of the code

3.2.1 Propagation of underwater focused ultrasound

Figures 2 and 3 show the computed results of propagating ultrasound in water medium. There are calculated by axisymmetric code. Three waves are generated. Figure 2 shows the pressure contour surface at the time just after releasing the third wave while Figure 3 does at the time of ultrasound focusing.

In Fig. 4, pressure distributions on the symmetry axis at various time steps are plotted. High pressure is obtained only near the focal point. Pressure level is over 10 times of the initial level at the focal point of focused ultrasound. The results show clearly the energy concentration at the geometric focal point.

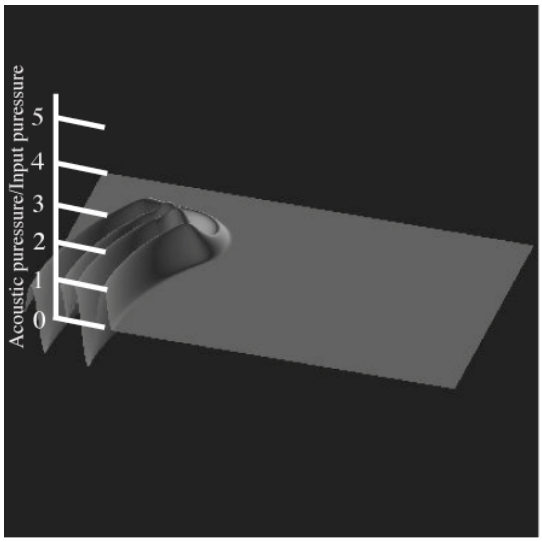

Figure 2: Pressure distribution in the plane just after ultrasound is generated

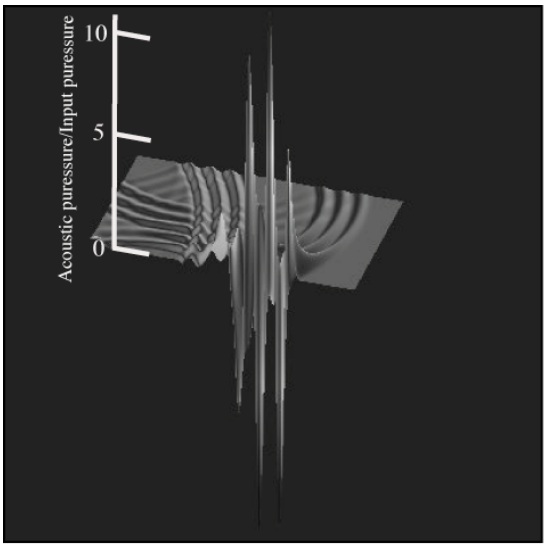

Figure 3: Pressure distribution in the plane when ultrasound is focusing

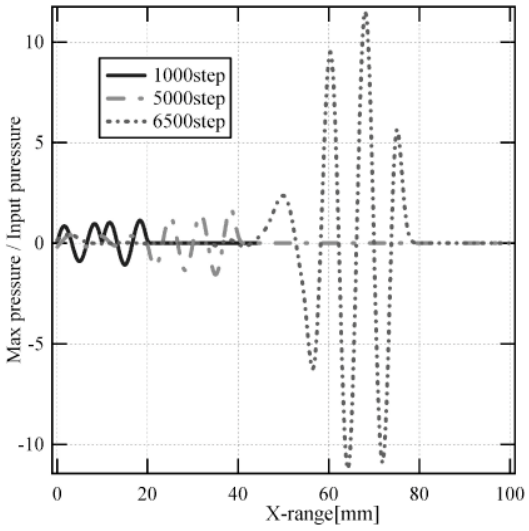

Figure 4: Sound pressure in each time step (1000,5000,6500)

3.3 Propagation of multi-media focused ultrasound

In order to verify the present code in different media, we perform the experiment and the computation of ultrasound wave propagation.

3.3.1 Experiment outline

Figure 5 is the outline of an experimental device. The function generator sends sine waves

to the amplifier. The amplified sine wave is sent to the hemispheric piezoelectric transducer (Fig. 6). Ultrasound wave is measured by ultrasound hydrophone and visualized by digital oscilloscope.

Speed of sound and the density of the media which are used in this research are normalized with the values of water, as shown in Table 1.

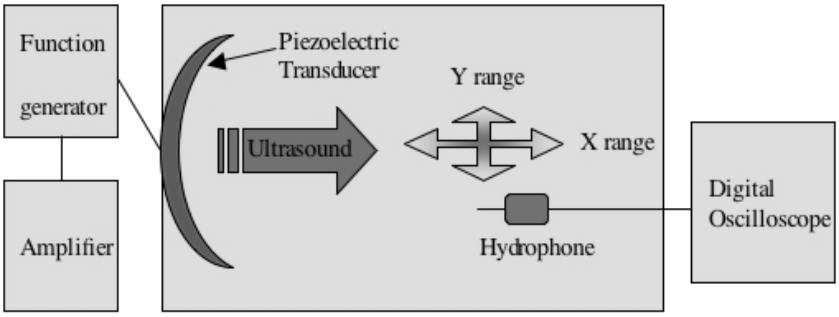

Figure 5: Density and the speed of sound

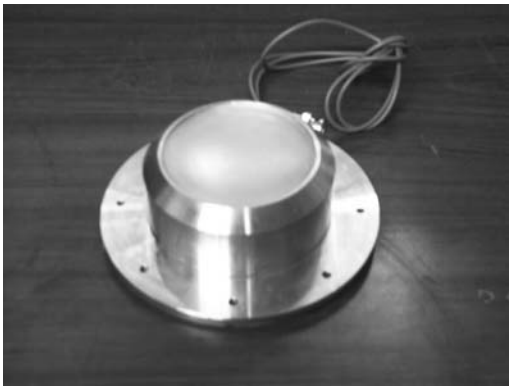

Figure 6: Piezoelectric transducer

	Speed of sound	Density	Acoustic impedance
Water	1.00	1.00	1.00
Acryl	1.84	1.20	2.21
Rubber	1.01	1.14	1.15
Duralumin	4.26	2.79	11.8

Table 1: Acoustic feature of each medium

3.3.2 Experiment result for different media

Figure 7 shows the experimental result of the present model. Used frequency is 2.14MHz. Result of the acoustic pressure distribution on the X-axis is plotted.

(a) No obstacle (water)

The ultrasound wave focuses at the geometric focal point of the ultrasound generator. The peak pressure is observed at that point.

(b) Acryl

Focal position moves forward (-x direction). Focal pressure is lower compared with water. It is due to the acoustic speed and sound impedance of acrylic obstacle.

(c) Rubber

Focal position hardly changes. However, the focal pressure is lower compared with water. It is because the elasticity of rubber may dump the propagating ultrasound.

(d) Duralumin

The focal point moves forward most among these cases. Also the peak pressure is lowest.

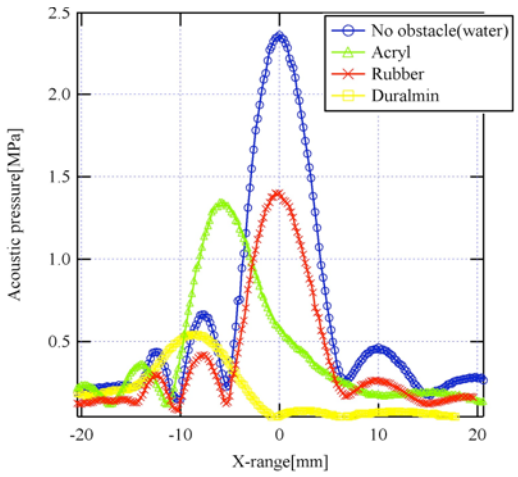

Figure 7: Experimental result of multi-media model

3.3.3 Numerical result for different media

The results for the experimental model are shown in Fig. 8. Frequency is 0.55MHz. The maximum value at each grid point on the X-axis throughout the computation is plotted. When focal area define half of maximum pressure.

(a) No obstacle (water)

Ultrasound wave converges at the geometric focus. The sound pressure at the focus is the highest and focal area is 28.6mm.

(b) Acryl

The focal point of ultrasound wave moves by 6.0[mm] to ultrasound generating point. Reflection occurs on the boundary of water and acryl. Thus, the sound pressure at the focus is smaller than that of water.

(c) Rubber

Sound speed and density of rubber are close to those of water. Thus, Sound pressure distribution is almost the same as water.

(d) Duralmin

Duralmin has very high speed of sound and density. Thus, The focal point of ultrasound wave moves by 10.8[mm] to ultrasound generating point and the peak pressure is lowest.

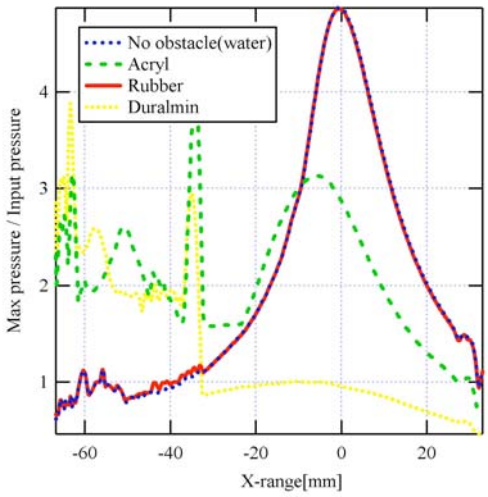

Figure 8: Calculation result of multi-media model

3.3.4 Comparison of simulation with experiment

Table 2 summarizes the comparison of numerical simulation results with experiment results where “obstacle” indicates each medium, “axis” indicates direction of axis, “focal area” indicates length of focal area, and “focal points” indicates distance from focal point of water condition.

For focal point, experiments and numerical result almost have the same values.

For focal area, each focal area agrees well, if focal area is inversely proportional to frequency. In general, the resolution of an ultrasound wave is expressed as $dx=c/f$ where dx is resolution, c is speed of sound and f is frequency.

Thus, calculation results and experiment results are quantitatively agreed and the present code was validated for ultrasound propagation in multi-media.

Experimental results				Numerical results			
Frequency	2.14MHz			Frequency	0.55MHz		
Obstacle	Axis	Focal area	Focal points	Obstacle	Axis	Focal area	Focal points
Water	x	7.2[mm]	-	Water	x	28.6[mm]	-
	y	1.0[mm]	-		y	3.6[mm]	-
Acrylic	x	8.0 [mm]	-6.2[mm]	Acrylic	x	38.4 [mm]	-6.0[mm]
	y	1.0[mm]	-		y	4.6[mm]	-
Rubber	x	7.0[mm]	-0.0[mm]	Rubber	x	28.6[mm]	-0.0[mm]
	y	1.0[mm]	-		y	3.6[mm]	-
Duralumin	x	9.6[mm]	-8.2[mm]	Duralumin	x	-	-10.8[mm]
	y	1.0[mm]	-		y	4.6[mm]	-

Table 2: Comparison of simulation result with experiment (multi-media)

3.4 Focused ultrasound of realistic frequency

In order to use realistic frequency, parallel computing was performed. Grid point is 4000 ×2000 and used frequency is 2.2MHz with axisymmetric code. One period of a wave is expressed with 20 grid points.

The result for this realistic frequency is shown in Fig. 9. The maximum value at each grid point on axisymmetric plane throughout the computation is plotted.

Pressure distributions at numerical simulation and experiment are shown in Fig. 10. Figure 10 shows that experimental result and numerical result are in good agreement at form of focal area, position of side lobe.

Thus, the present code was validated at realistic frequency focused ultrasound.

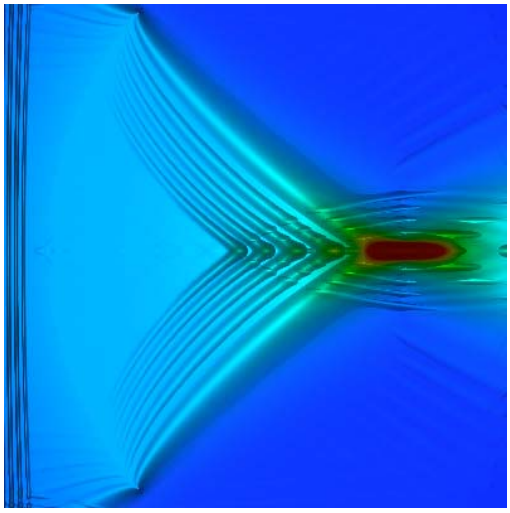

Figure 9: Simulation result of sound pressure distribution using 2.2MHz ultrasound

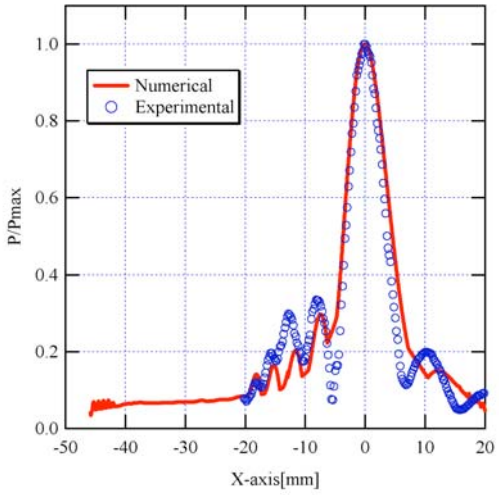

Figure 10: Pressure distribution in numerical simulation and experiment

3.5 Three dimensional focused ultrasound

The present technique was verified in the previous section. However, three-dimensional form of body tissue is not expressed with axisymmetric assumption. Thus, three-dimensional calculation code, which can express arbitrary form, was developed.

Figure 11 shows ultrasound wave focusing in three dimensions. Figure 12 shows the ultrasound wave passing though at acryl board. Reflecting of ultrasound at acryl board, and phase lag at focal area are observed.

It is concluded that the present method can expressed arbitrary shape media.

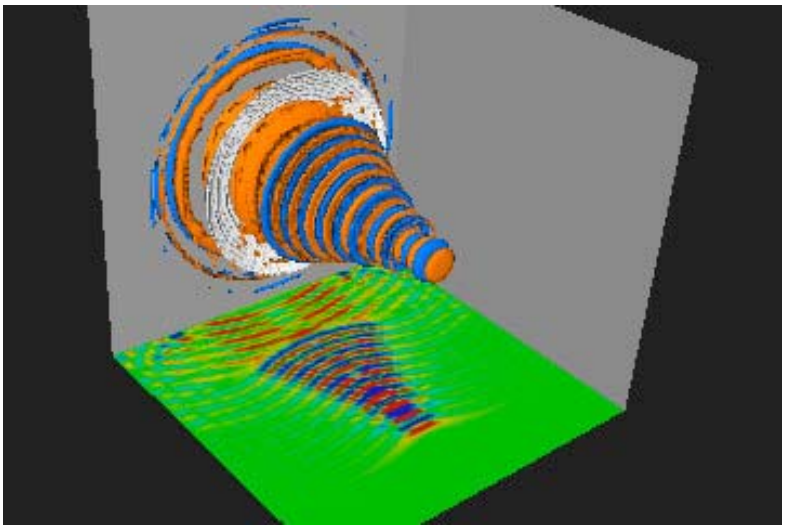

Figure 11: Focusing of ultrasound using three-dimensional code (No obstacle condition)

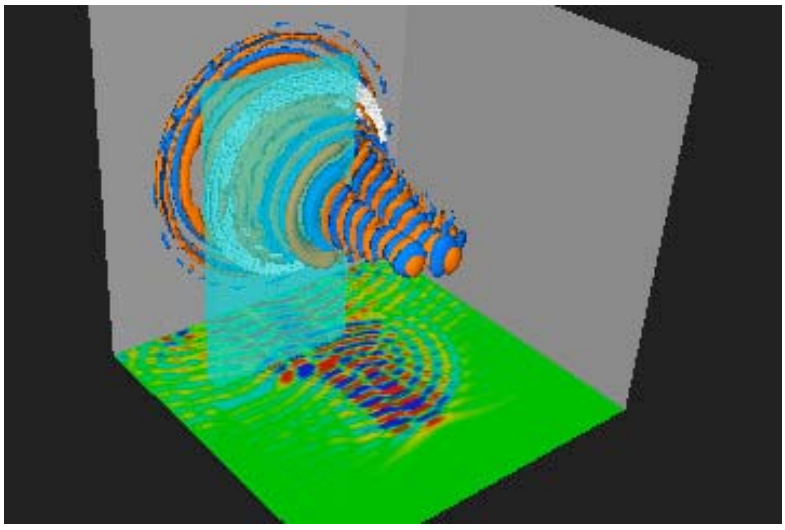

Figure 12: Focusing of ultrasound using three-dimensional code (Acryl at light blue area)

4 TRANSSKULL FOCUSED ULTRASOUND

4.1 Acoustic feature of the skull from CT scan data

The present method is expressed arbitrary shape media in the previous section. In this section, we used CT scan data to make skull model. Figure 13 shows that CT scan of three-dimensional skull used in this research.

CT scan image is used to measure internal density of skull. Skull has various density and speed of sound. The skull has three-layered structure, structure of porous zone layer, and dense layers. Structure of porous zone is very inhomogeneous. Acoustic feature of water and skull used in this study is shown in the Table 2.

The porosity map is directly linked to CT scan data, called Hounsfield value.

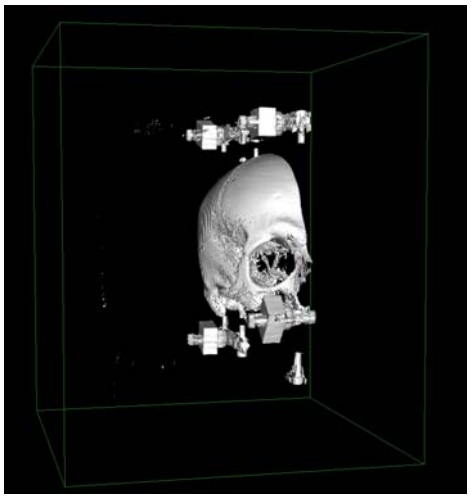

Figure 13: Computerized tomography scan of three-dimensional skull

Actual process of making skull model from CT scan data is as follows.

(a) The Hounsfield value is defined by eq. (4) where μ_x is absorption coefficient of X-ray at each point, μ_{water} is water absorption coefficient of X-ray, μ_{bone} is bone absorption coefficient.
(b) Data of calculation area is extracted.
(c) Porosity distribution Φ is derived from Hounsfield value distribution by eq. (5).
(d) Speed of sound is defined by eq. (6).
(e) Density is defined by eq. (7)

$$H = 1000 \frac{\mu_x - \mu_{water}}{\mu_{bone} - \mu_{water}} \tag{4}$$

$$\Phi = 1 - \frac{H}{1000} \tag{5}$$

$$c = c_{water} + (c_{bone} - c_{water}) \times (1 - \Phi) \tag{6}$$

$$\rho = \Phi \times \rho_{water} + (1 - \Phi) \times \rho_{bone} \tag{7}$$

	Speed of sound [m/s]	Density [Kg/m^3]
Water	1500	1000
Skull	2900	1900

Table 3: Acoustic feature of water and skull

Figure 15 shows porosity distribution derived from slice of CT scan data (Fig. 14). As skull consists of porous medium, skull bone is inhomogeneous to the ultrasound waves. Figure 16 shows speed of sound and density distribution. Skull bone has a broad range of sound of speed and density.

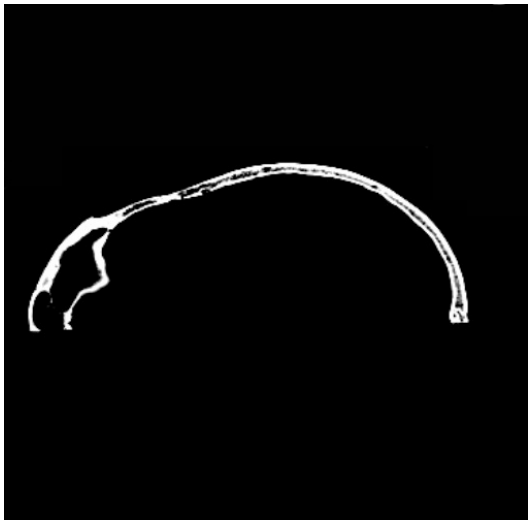

Figure 14: Slice of the three-dimensional skull data used by calculation

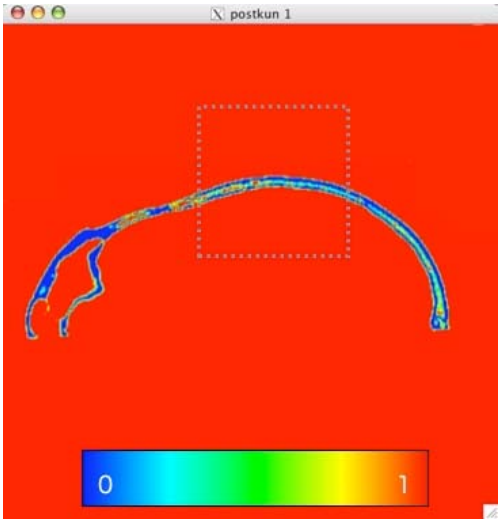

Figure 15: Porosity distribution of slice of the skull

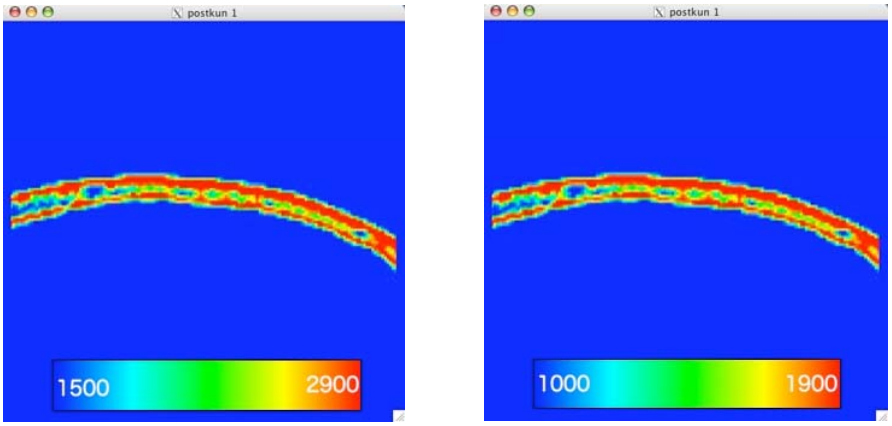

Speed of sound distribution [m/s] Density distribution [Kgm^{-3}]

Figure 16: acoustic feature of slice of skull

4.2 Simulation of transskull focused ultrasound

Grid point is 500×500 and used frequency is 0.55MHz with two-dimensional code. Figure 8 to 10 show acoustic pressure at ultrasound generation, at passing through skull, at having passed through skull respectively. Additionally, bone position is superposed.

Figure 17 shows that generated ultrasound waves are conversing at the geometric focal point. Because of the effect of skull, ultrasound waves are reflected and refracted on the skull (Fig. 18). Then, focal point of the ultrasound is changed, and acoustic pressure in focal point is observed lower (Fig. 19).

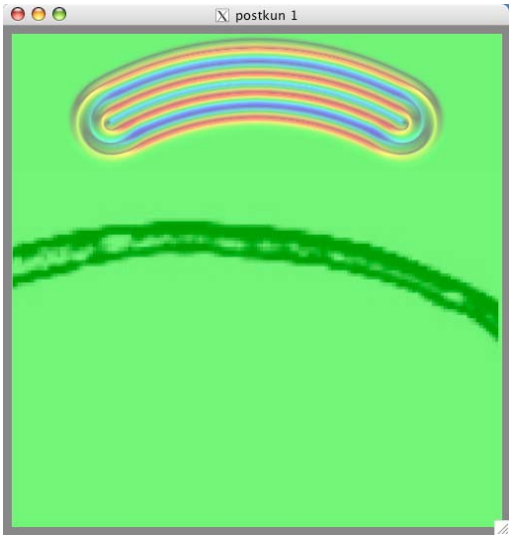

Figure 17: Sound pressure distribution at generating ultrasound

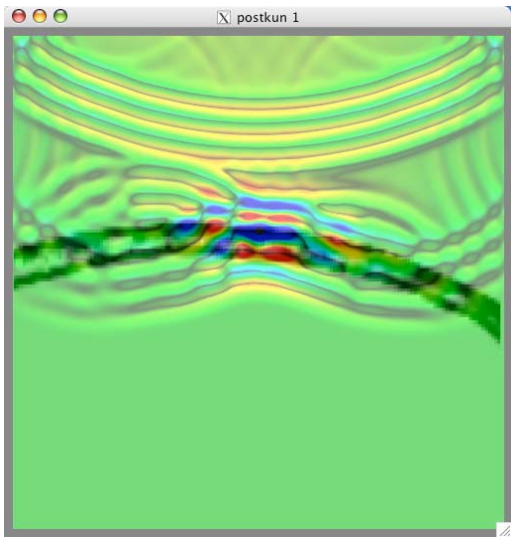

Figure 18: Sound pressure distribution at passing through skull

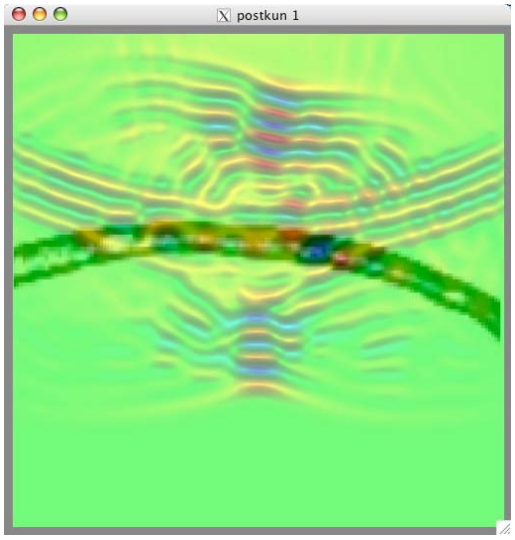

Figure 19: Sound pressure distribution at having passed through skull

In order to illustrate the depth of the focal point, Figure 20 and 21 show the image of the two dimensional result, which is three dimensionally superposed on the skull model.

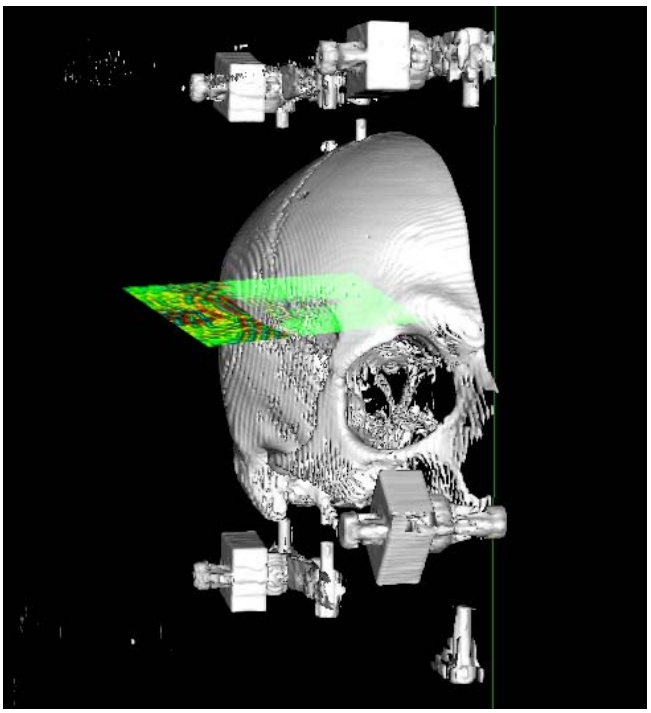

Figure 20: Two-dimensional ultrasound passing through skull

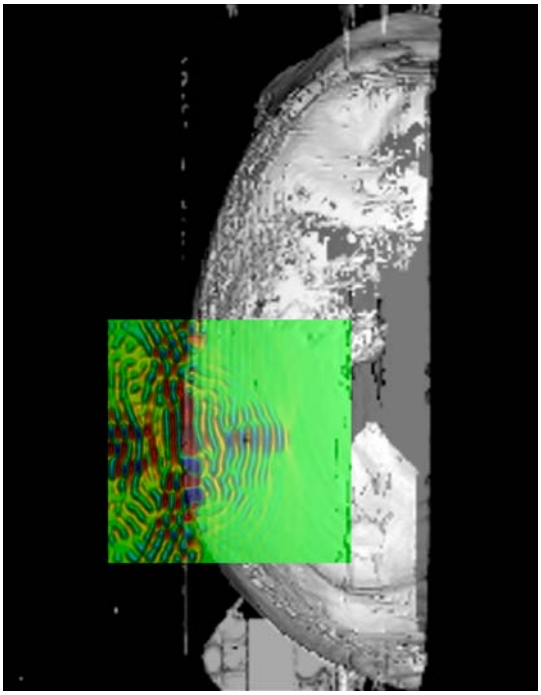

Figure 21: Slice of two dimensional ultrasound passing through skull

5 CONCLUSIONS

In order to apply HIFU treatment to brain, we proposed analysis transskull focused ultrasound. Skull model is made by CT scan data for apply to calculation.

- We simulate focused ultrasound of real frequency (used by experiment) by parallel computing. Sound pressure distribution of focal area shows good agreement with experiment.
- The propagation, reflection, and refraction of the ultrasound waves which passes through passed multi-media agreed with experiment.
- Three-dimensional parallel computing code for realistic three-dimensional setup is developed.
- We made skull model using CT data by the consider relation between Hounsfield value and porosity.
- Two-dimensional focused ultrasound passing through skull is simulated. Ultrasound wave reflects and refracts according to acoustic future of skull.

ACKNOWLEDGEMENT

Authors thank Professor M. Fink and Dr. J. -F. Aubry of Ecole Supérieure de Physique et Chimie Industrielles de la Ville de Paris for their courtesy of three dimensional CT scan data.

REFERENCES

[1] ter Haar, G “Acoustic surgery”, Physics Today, Vol. 54, Issue 12, pp.29-34, (2001)
[2] Matsumoto, Kennedy, J.E, et al., “High-intensity focused ultrasound for the treatment of liver tumors”, Ultrasonics, Vol. 42, Issue 1-9, pp.931-936, (2004)
[3] Y. Matsumoto, et al., “Medical ultrasound with microbubbles”, Experimental Thermal and Fluid Science, Vol. 29, pp.255-265, (2005)
[4] J. -F. Aubry, et al., “Experimental demonstration of non invasive transskull adaptive focusing based on prior CT scans”, The Journal of the Acoustical Society of America, Vol. 113, Issue 1, pp. 84-93, (2003)
[5] J. Y. Rho, et al., “Relations of mechanical properties to density and CT numbers in human bone”, Medical Engineering & Physics, Volume 17, Issue 5, pp323-399, (1995)